

# Wave Friction Factors from Energy Flux Comparisons Outside of the Surf Zone

Jodi L. Eshleman<sup>†</sup>, Robert G. Dean<sup>‡</sup>, and Kent K. Hathaway<sup>§</sup>

<sup>†</sup>University of Florida  
Civil and Coastal Engineering  
Department  
554 Weil Hall  
Gainesville, FL 32611-6590,  
U.S.A.  
jeshleman@usgs.gov

<sup>‡</sup>Graduate Research Professor  
(Emeritus)  
University of Florida  
Civil and Coastal Engineering  
Department  
575 H Weil Hall  
Gainesville, FL 32611-6590,  
U.S.A.

<sup>§</sup>Research Oceanographer  
Coastal and Hydraulics  
Laboratory  
Field Research Facility  
1261 Duck Rd.  
Kitty Hawk, NC 27949,  
U.S.A.

## ABSTRACT

ESHLEMAN, J.L.; DEAN, R.G., and HATHAWAY, K.K., 2006. Wave friction factors from energy flux comparisons outside of the surf zone. *Journal of Coastal Research*, 22(6), 1490–1498. West Palm Beach (Florida), ISSN 0749-0208.

Pressure, sonar profiling, and current measurements were recorded at 5.5-, 8-, and 13-m water depths in the outer surf zone and inner continental shelf region off the coast of Duck, North Carolina. This unique data set was analyzed to investigate wave evolution by comparing estimates from linear wave theory with field measurements. Energy flux calculations combining shoaling and refraction theory showed smaller measured than predicted energy flux values at the two inshore locations (sometimes by more than one third), emphasizing the importance of considering energy loss in engineering design and planning calculations. A wave friction factor for each record was determined by accounting for frictional energy loss in the energy flux calculation, using velocity time series measured 0.20, 0.55, and 1.50 m above the sea floor. Calculated friction factors varied throughout storm events, but most fell within a range of 0 to 0.1. Wave friction factors calculated using the total measured velocity time series showed a narrower range (0 to 0.05) than those calculated from demeaned velocities (0 to 0.1). Representative wave friction factors of 0.053 (demeaned velocity) and 0.0209 (total velocity) were identified for this location using a least squares fit between energy flux decay and  $|u_x|^3 \Delta x$  over all storm events.

**ADDITIONAL INDEX WORDS:** *Wave shoaling, energy dissipation, nearshore, energy flux*



## INTRODUCTION

The inner continental shelf of the open mid-Atlantic coast is a wave-driven environment, where sediment transport and nearshore circulation are primarily forced by wind-generated ocean surface waves (WRIGHT, 1995). This is a friction-dominated region where wave propagation is largely characterized by transformation through refraction, diffraction, energy dissipation, and shoaling. Standard small-amplitude wave theory assumes irrotational flow, and an impermeable and horizontal bottom, which is not realistic in a natural setting (DEAN and DALRYMPLE, 1991). Waves propagating over real seabeds will be affected by bottom slope, and bottom surface roughness and permeability. The waves will also experience energy dissipation from bottom friction, due to nonlinear shear stresses created by a turbulent boundary layer at the bottom (DEAN and DALRYMPLE, 1991). White capping and flow through the permeable medium are additional mechanisms of energy loss, considered here to be secondary to bottom friction.

### Background

Significant efforts have been directed toward determining friction factors based on bottom velocity measurements.

JONSSON (1966) related the friction factor to maximum bed shear stress and developed relationships with Reynolds number and bottom roughness parameters. MADSEN *et al.* (1988) give explicit formulas for wave friction factors that are dependent on the relative magnitude of the current shear stress. YOUNG and GORMAN (1995) utilized the WAM model to account for other dissipation by comparing measured and calculated wave spectra to determine best-fit friction factor values. NELSON (1996) calculated bed roughness values for an offshore reef by investigating wave attenuation in a swell dominated environment. Several recent studies have used turbulence measurements to determine near-bottom turbulent shear stress and friction factors (SMYTH and HAY, 2002; 2003; TREMBANIS *et al.*, 2004). Another approach recently employed by TREMBANIS *et al.* was to use the inertial dissipation method to estimate the combined wave-current shear velocity, which is then used to determine a wave friction factor. Although accomplished through many different computational techniques, they all account for wave energy dissipation by friction.

The focus of this study was to calculate energy fluxes based on current and pressure measurements collected at three different water depths and subsequently to determine a representative wave friction factor for this location in Duck, North Carolina. The analysis applies an energy conservation approach to develop friction factors.

## FIELD MEASUREMENTS

### Geographic Location

Field data were obtained on the inner continental shelf off the coast of the U. S. Corps of Engineers Field Research Facility (FRF). The FRF facility is located on the Outer Banks of North Carolina, on the central portion of the Currituck Spit, which extends southeast continuously for over 100 km from Cape Henry, Virginia, to Oregon Inlet, North Carolina (Figure 1). It is located in the southern portion of the Middle Atlantic Bight (36°10'57"N; 75°45'50"W) and bordered by Currituck Sound, a low-salinity estuarine environment, on the west and the Atlantic Ocean on the east. Ocean tides are semidiurnal, with a mean range of approximately 1 m (BIRKEMEIER *et al.*, 1981).

### Bipod Instrumentation

Three instrumented bipods were deployed at nominal depths of 5.5, 8, and 13 m (Figure 2) in October of 1997 and remained operational through December of 1998. The instrumentation consisted of sensors, which were attached to the bipod frames, secured by two 6.4-m pipes jetted vertically into the seabed (BEAVERS, 1999). Each bipod package contained three SonTek Acoustic Doppler Velocimeters (ADV), which sampled at 2 Hz and were located at nominal elevations of 0.20, 0.55, and 1.50 m above the seafloor (Figure 3). The end of the frame containing the current meters was oriented toward the southeast to minimize interference of current meters and vertical supports with orbital velocities because storm events of interest would have primarily northeast waves (BEAVERS, 1999). Digital Paroscientific pressure gauges operating near a 38-kHz range were sampled with a 50-ms integration at 2 Hz. Each bipod had a Datasonics sonar altimeter (Model SA900) that measured changes in bed elevation, sampling at 1 Hz and approximately 1 cm accuracy.

### Data

The analysis focuses on estimates of wave direction, transformation, and energy dissipation during storm conditions at a longshore position approximately 400 m north of the FRF pier. The data set consists of current and pressure measurements recorded in three different water depths (nominally 5.5, 8, and 13 m), which are located at approximately the same long-shore position, thus establishing a cross-shore array of instrumentation. Choosing records from the data set that contain significant energy enhances the significance of the results. The following analysis is based on 4 months during which data quality standards were satisfied: October 1997, November 1997, May 1998, and August 1998. There are six significant storm events that occurred within this 4-month period. The range of significant wave heights included in this analysis is  $1.75 \text{ m} < H_s < 3.5 \text{ m}$ .

Wave refraction calculations used Snell's Law and assumed that the bathymetry consisted of straight and parallel bottom contours. The bipods are located in an area where this assumption is reasonable. Figure 2 presents profiles in the area around the time that these data were collected and the solid dots represent the approximate locations of the 5.5-, 8-, and

13-m bipods. These profiles were measured at the FRF using the Coastal Research Amphibious Buggy (CRAB) and the Lighter Amphibious Resupply Cargo (LARC). Wave calculations include data within the frequency range of 0.05 to 0.2 Hz, which corresponds to the frequency range of significant energy evident from pressure measurements. The high-frequency cutoff of 0.2 Hz (5-second period) is chosen because shorter period waves would be close to the deep water range at the 13-m location and would neither affect the bottom nor be readily measurable because of low-pressure signals.

## RESULTS

### Development of Directional Spectra

Directional spectral estimates were developed from the measured pressures and velocity components during significant storm events using the p-u-v method, which follows the work of LONGUET-HIGGINS *et al.* (1963). For simplicity, this analysis considers the pressure sensor and current meter to be located at the same horizontal location and distance above the bottom. The actual horizontal separation distance between the pressure and current meters is 0.56 m and the vertical separation distance is 0.22 m. A 10-second wave would have a wavelength of 71 m at the 5.5-m bipod, which is much larger than the separation distances, and the bipod NW-SE orientation justifies this horizontal collocated assumption. The auto and cross spectra were calculated with a segment length of  $N = 128$ , which yields a resolution of 0.015 Hz and 64 degrees of freedom. The actual number of degrees of freedom is somewhat greater because half-lapped segments are used.

### Energy Flux Calculations

Onshore energy flux  $\mathfrak{S}(f)$ , is defined as a function of frequency:

$$\mathfrak{S}(f) = \rho g S_{\eta\eta}(f) C_g(f) \cos \theta_m(f) \quad (1)$$

where  $\rho$  is the water mass density,  $g$  is gravity,  $S_{\eta\eta}$  is the spectral density, and  $C_g$  is the group velocity. The peak measured wave direction ( $\theta_m$ ) for each frequency to be used in calculations is taken as the direction of the maximum value in the computed directional spectrum. A calculated water surface spectrum was obtained at the 8-m inshore bipod location using the equation:

$$S_{\eta\eta c(8)}(f) = S_{\eta\eta m(13)}(f) \left[ \frac{C_{g(13)}(f)}{C_{g(8)}(f)} \right] \left[ \frac{\cos \theta_{m(13)}(f)}{\cos \theta_{c(8)}(f)} \right] \quad (2)$$

and similarly for the 5.5-m inshore bipod. In the previous equation, the calculated wave direction is defined from Snell's Law as:

$$\theta_{c(8)}(f) = \sin^{-1} \left[ \frac{C_{(8)}(f) \sin \theta_{m(13)}(f)}{C_{(13)}(f)} \right] \quad (3)$$

The use of  $\theta_m$  as the direction of the maximum value of the computed directional spectrum for each frequency leads to slightly larger energy flux values than if the entire range of directions was considered.

Figure 4 includes the total energy flux at each bipod loca-



Figure 1. Satellite image showing the location of the field research facility on the Outer Banks of North Carolina.

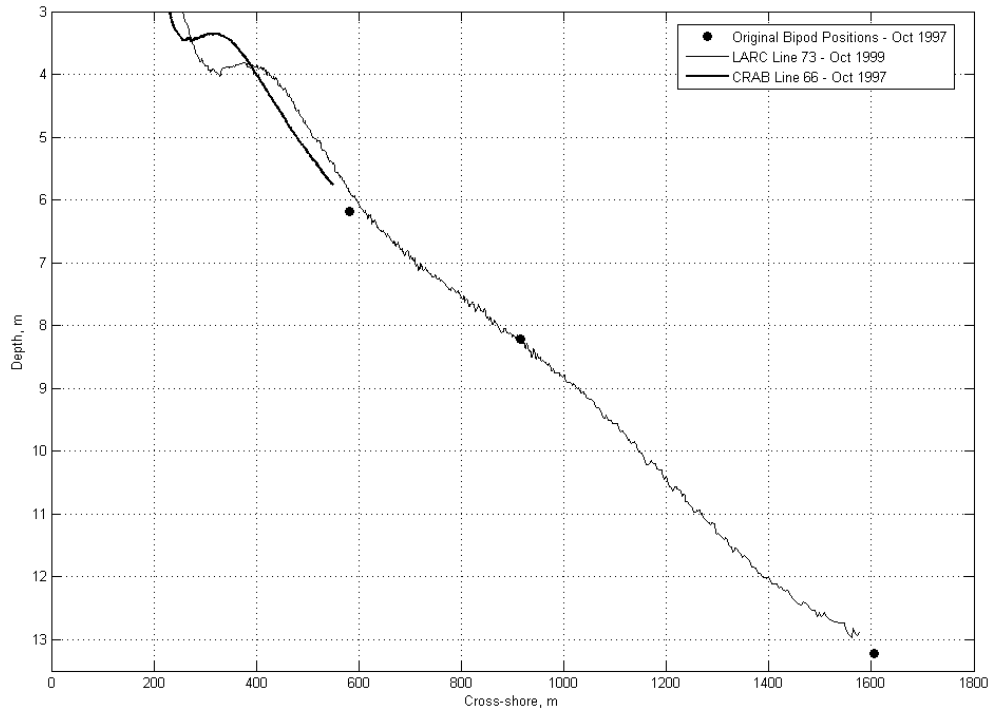


Figure 2. Surveyed profiles in vicinity of bipod instrumentation. Black circles indicate original bipod positions. Bold line shows survey data from this same month. Solid line shows the nearest available survey data out to 13-m water depth.

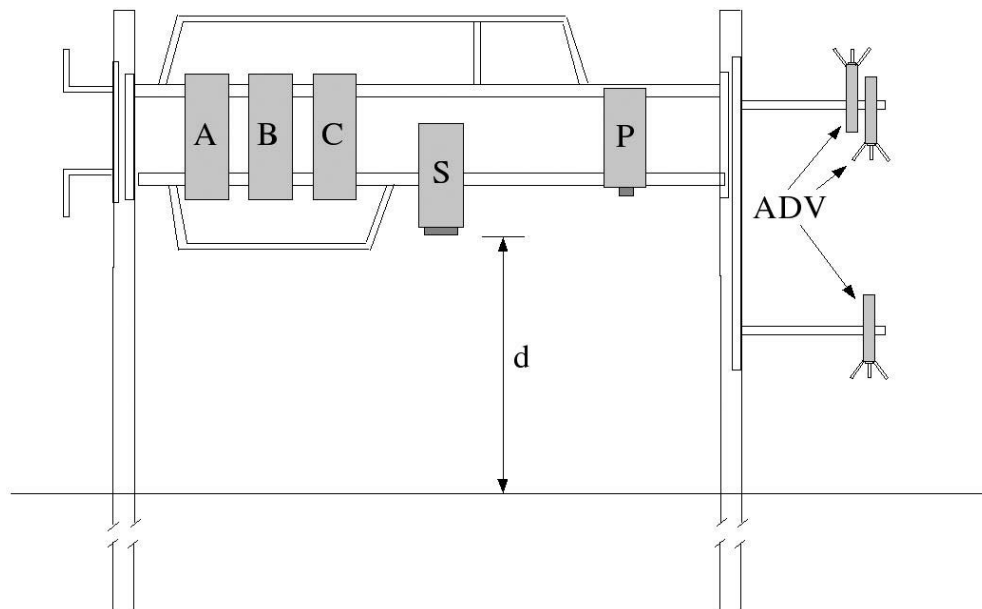


Figure 3. Bipod instrumentation. A,B,C indicate electronic housings, P is pressure sensor, and S is sonar altimeter.

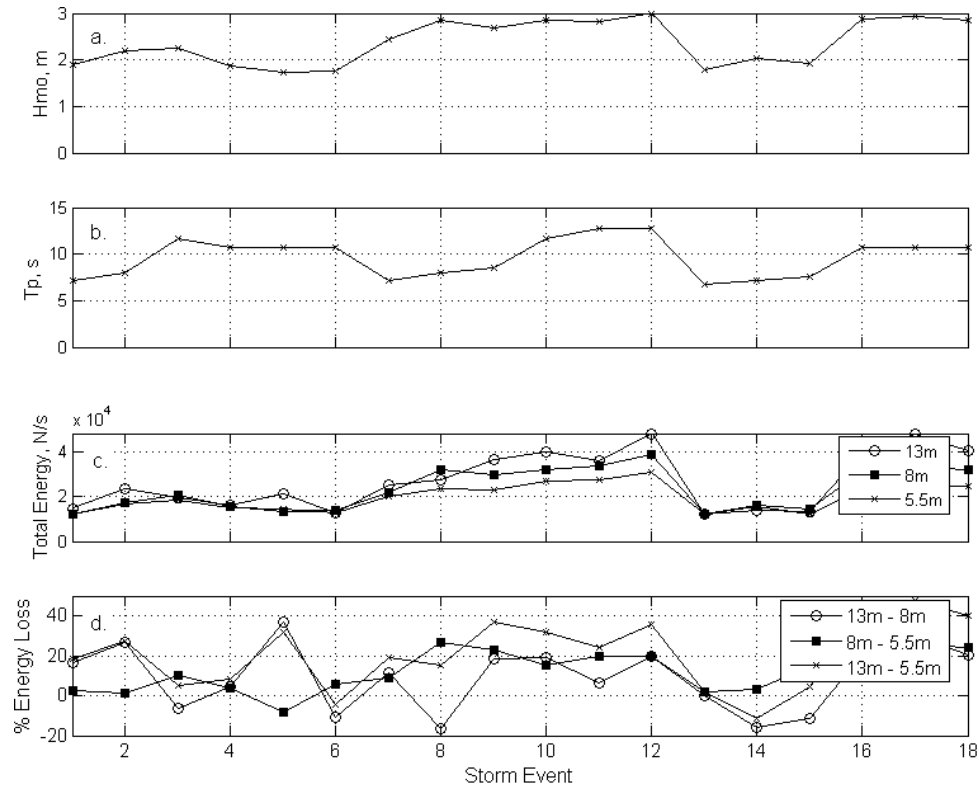


Figure 4. (a) Significant wave height, m, (b) peak wave period, s, (c) total energy flux, and (d) percent energy loss between bipods for each storm event.

tion and the percent energy loss (as a percentage of the offshore total energy flux value) between water depths for each storm event considered. The negative percent energy loss values indicate times when there was a larger wave height measured at the inshore bipod than predicted from linear wave theory calculations. One explanation for this is the possibility of energy growth due to wind. The largest negative values at storm events 8, 14, and 15 represent onshore directed winds ranging from 10 to 14 m/s. Some energy loss values are greater than 40% of the total energy flux.

Figure 5 shows the average energy flux variation over frequency range for all 18 storm events, and includes percent reduction in average energy fluxes. The dashed lines in plots 5b and 5c represent the calculated energy flux at the offshore bipod (13 m), which is the same as that predicted with no energy losses. These are compared with the measured values shown by the solid lines. The cross-shore separation distances between the three bipods differ. The 13- and 8-m bipods are separated by 690 m in the cross-shore direction and the 8- and 5.5-m bipods are separated by only 333 m. Of interest is that the average energy losses between the 8- and 5.5-m bipods are greater than between the 13- and 8-m bipods (Figure 5), even though the separation distance for the 13- and 8-m bipods is twice as great. Of course, the reason is that bottom friction is more effective in causing energy losses in shallower water.

**Friction Factor**

This analysis assumes that friction is the only cause of energy change between bipods. In reality there are many other contributing factors, including the possibility of energy growth due to wind, energy loss due to white capping, or the redistribution of energy within the spectrum due to nonlinear interactions, *etc.* By accounting for frictional energy loss in the energy flux calculation, we can determine a wave friction factor.

The friction factor is estimated using:

$$\int_{0.05 \text{ Hz}}^{0.2 \text{ Hz}} \mathfrak{S}_a df - \int_{0.05 \text{ Hz}}^{0.2 \text{ Hz}} \mathfrak{S}_b df = \frac{1}{2}[\varepsilon_{Da} + \varepsilon_{Db}]\Delta x_{a,b} \quad (4)$$

where the subscripts *a* and *b* denote bipod locations, and  $\Delta x_{a,b}$  is the total cross-shore distance between the *a* and *b* bipods.  $\varepsilon_D$  is the energy loss term expressed as:

$$\varepsilon_D = \overline{\vec{\tau}_b \cdot \vec{u}_b} = \rho C_f [u_{b,x}(t)^2 + u_{b,y}(t)^2]^{3/2} \quad (5)$$

in which  $u_{b,x}$  and  $u_{b,y}$  are the onshore and shore parallel components of bottom water particle velocity and:

$$\vec{u}_b = \vec{i}u_{b,x} + \vec{j}u_{b,y} \quad (6)$$

where  $\vec{i}$  and  $\vec{j}$  are the onshore and shore parallel unit vectors, respectively. Equation (5) accounts for energy damping by bottom friction, and  $C_f$  is the wave friction factor. The bottom shear stress,  $\vec{\tau}_b$ , is:

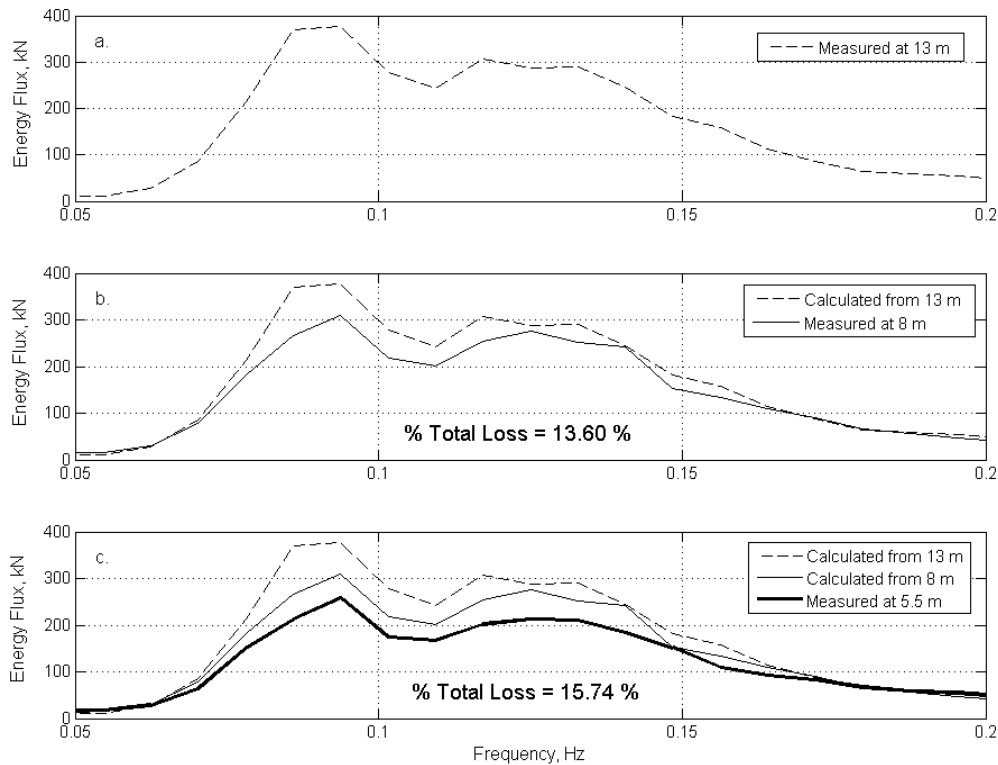


Figure 5. Average measured energy flux variation with frequency (Hz). (a) 13 m, (b) 8 m, and (c) 5.5 m. Averages represent all 18 data sets analyzed herein. Percentages represent energy losses between the bipod at that depth and the next seaward bipod.

$$\bar{\tau}_b = \rho C_f |\bar{u}_b| \bar{u}_b \tag{7}$$

The calculated friction factors of interest are those resulting from the wave component of velocity measurements from the bottom current meter because this velocity is the most

Table 1. Friction factor estimates from bottom current meter.

Date	$C_f$ (wave)	$C_f$ (Total)	$H_{mo}$
10/19/1997	0.0313	0.0129	1.89
10/19/1997	0.0507	0.0138	2.19
10/20/1997	0.0053	0.0032	2.24
11/7/1997	0.0111	0.0073	1.88
11/7/1997	0.0533	0.0355	1.73
11/8/1997	-0.0052	-0.0036	1.76
11/13/1997	0.0287	0.0195	2.43
11/13/1997	0.0209	0.013	2.84
11/13/1997	0.0602	0.0396	2.68
5/13/1998	0.0485	0.021	2.84
5/13/1998	0.0331	0.0118	2.83
5/13/1998	0.0557	0.0309	3.00
8/2/1998	0.0029	0.002	1.78
8/2/1998	-0.0141	-0.0103	2.02
8/2/1998	0.0072	0.005	1.91
8/27/1998	0.0704	0.0162	2.88
8/27/1998	0.0868	0.0222	2.93
8/27/1998	0.0639	0.0232	2.84
Average	0.0339	0.0146	2.37
Standard Deviation	0.0288	0.0131	0.48

representative of the bottom velocity. In the following analysis, we also include calculations using the total velocity time series for comparison because we can never actually separate the wave and current velocity effects on energy losses. The first form is referred to as “wave only” velocity, and this includes measured velocity time series that have been de-meaned and band-pass filtered to include only the frequency range from 0.05 to 0.2 Hz, because this is the range used in energy flux calculations. The second form is referred to as the “total” velocity, and it includes the total measured velocity time series.

Most “wave only” friction factor estimates from the bottom current meter are in the range of 0 to 0.1, although there are several negative values due to energy growth between bipods (Table 1). All friction factors included in Table 1 are determined from measurements recorded at the bottom current meter on the 13- and 5.5-m bipods. The mean and standard deviation for the “wave only”  $C_f$  values based on the bottom current meter are 0.0339 and 0.0288, respectively. The negative value on August 2, 1998, is probably a reflection of poor data quality, because the bottom current meter had a data quality flag for low beam correlation. The other current meters gave estimates on the order of 0.002 for this same date, which is more reasonable.

It does not seem unreasonable to find a range of  $C_f$  during storms and for different storm conditions because friction fac-

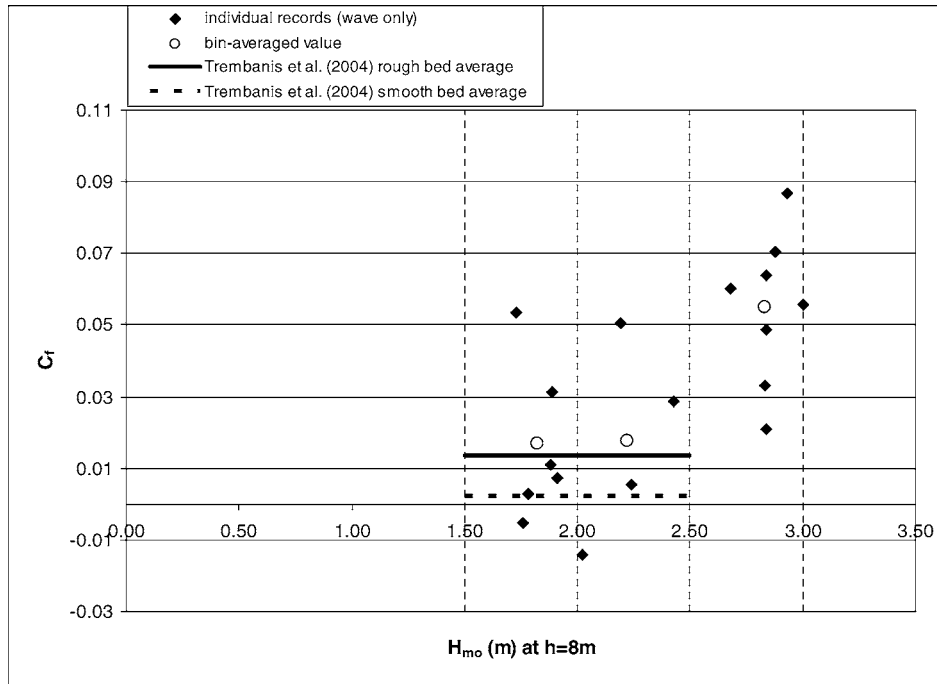


Figure 6. Friction factor variation with wave height at the bottom current meter. The bin-averaged values are the results of averaging friction factors over the 0.5-m wave height ranges shown by the vertical dashed lines. Average values of  $f_w$  from Trembanis *et al.* (2004) are calculated from field measurements in New Zealand in 15 to 20 m of water and have been converted to  $C_f$  from ( $C_f = 1/2f_w$ ).

tors can change as currents increase and bottom conditions (roughness) change. Figure 6 shows that friction factors generally increase with significant wave heights. Figure 6 also presents bin-averaged values of friction factors, which are av-

eraged over the 0.5-m wave height intervals shown by the vertical dashed lines. It is important to note that if the highest waves were breaking (turbulent dissipation) before reaching the 5.5-m bipod, the friction factors would be unrealisti-

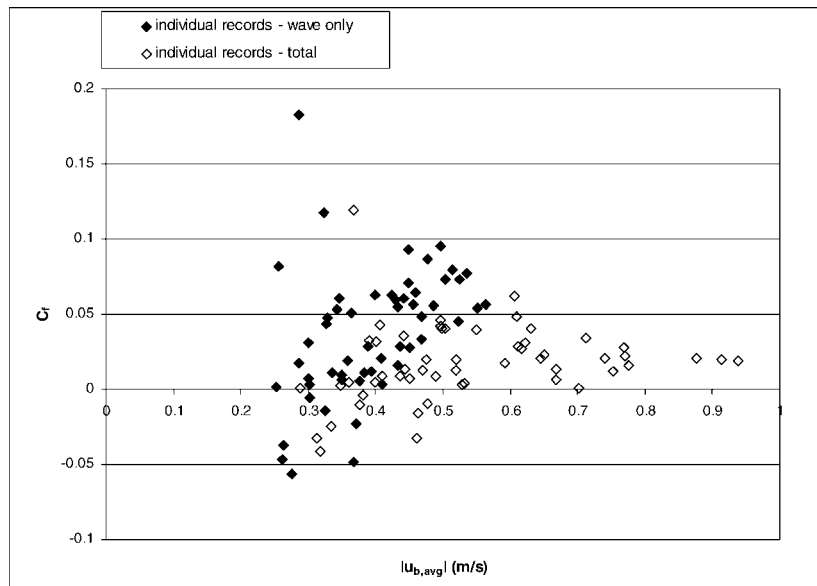


Figure 7. Friction factor variation with bottom velocity. Estimates using data between 13–5.5 m, 13–8 m, and 8–5.5 m are included.

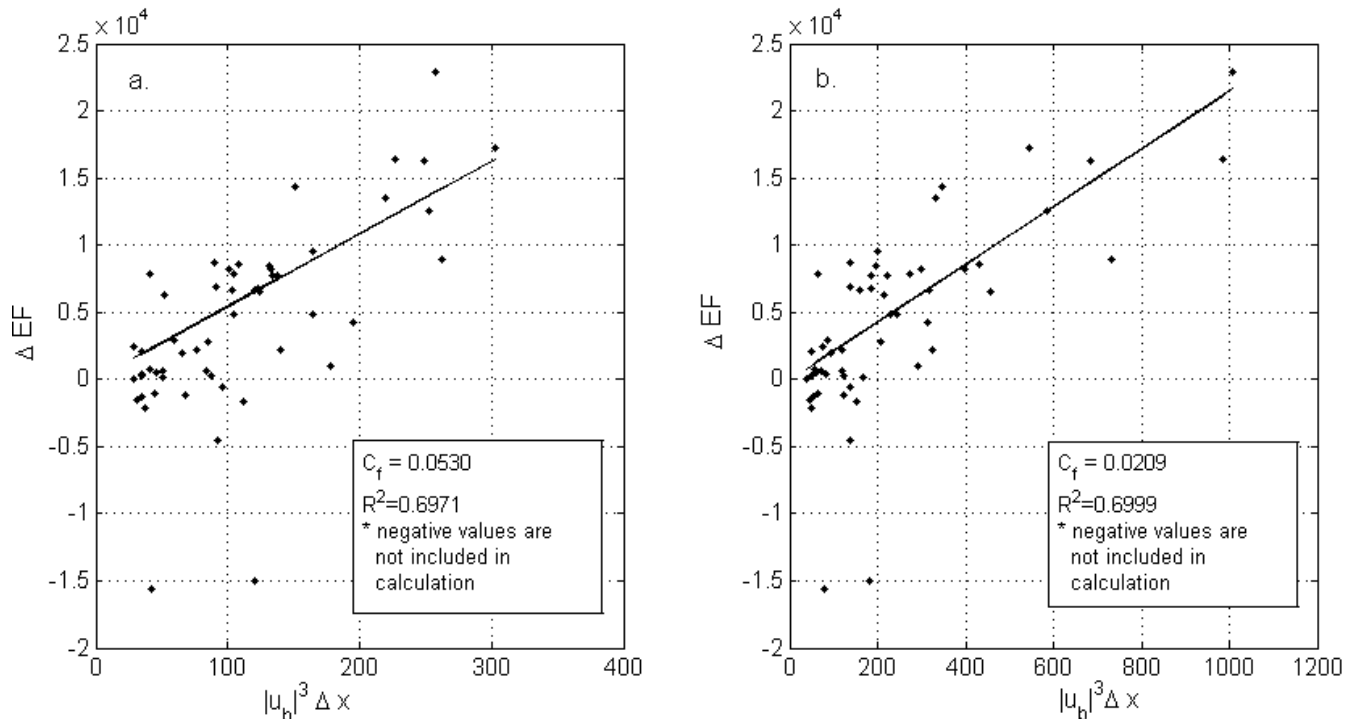


Figure 8. Correlation plots between energy flux decay and  $|u_b|^3 \Delta x$  for (a) wave only and (b) total velocity. Both correlation coefficients are significant at the 99% confidence level.

cally high because the calculation methodology assumes that all energy dissipation is from bottom friction. The bin-averaged values show a sharp jump for the 2.5- to 3-m wave height bin, suggesting that the increase may be a result of waves breaking at the 5.5-m bipod. In order to test this case, we calculated these same friction factors using only data from the 13- and 8-m bipods. This dropped the third bin-averaged value to 0.0445, which is still significantly higher than the other two.

Comparisons of wave friction factors with other studies show values on the same order of magnitude. The horizontal lines in Figure 6 represent values calculated by TREMBANIS *et al.* (2003) for similar water depths at a location in New Zealand. They calculated average values for a range of wave conditions, and these values fall within the range of values determined here. SMYTH and HAY (2003) calculated friction factors from data collected in shallower water (3.5 m) at Duck, North Carolina. They found  $f_w$  values ranging from 0.0042 to 0.079, which correspond to  $C_f$  values ranging from 0.0021 to 0.0395. Friction factor estimates from the higher current meter data used in the present study were found to be consistent with those based on the lower current meter. Figure 7 includes all “wave only” and “total” velocity friction factors plotted *vs.* bottom velocity. These show an increase with bottom velocity. The friction factors calculated from “total” velocity show a narrower range (0 to 0.05) than those determined from the “wave only” velocity (0 to 0.1).

To improve stability in the friction factor estimates, a single representative wave friction factor for this specific loca-

tion was determined using a least squares fit between energy flux decay and  $|u_b|^3 \Delta x$ . Including  $\Delta x$  in this formulation allowed the use of friction factors calculated between 13 and 8 m, 8 and 5.5 m, and 13 and 5.5 m. A  $C_f$  value of 0.0530 was determined for the “wave only” calculation and 0.0209 for “total” velocity. Figure 8 presents correlation plots between energy flux decay and  $|u_b|^3 \Delta x$ . The “wave only” and “total” velocity calculations gave very similar correlation coefficients of about 0.70, significant at the 99% confidence level.

## CONCLUSIONS

Energy flux calculations combining shoaling and refraction theory showed smaller measured than predicted energy flux values with inshore distance, reflecting energy loss processes. The energy loss reached more than 40% on the inner continental shelf, emphasizing the importance of considering energy loss in engineering design and planning calculations. Wave friction factors were estimated by accounting for energy losses, and most values fell in the range of 0 to 0.1, although these tend to vary with storm conditions. Using a single friction factor of 0.01 seems reasonable if there are no measurements of roughness, but it may underestimate losses during high energy events where estimates can be up to an order of magnitude higher. Calculations utilizing the total measured velocity show a narrower range of values than those that attempt to isolate the wave component, but both show a similar correlation between energy flux decay and  $|u_b|^3 \Delta x$ . Representative wave friction factors of 0.053 (wave only) and

0.0209 (total) were identified for this location using a least squares fit between energy flux decay and  $|u_b|^3 \Delta x$ .

### ACKNOWLEDGMENTS

The research presented in this paper was conducted under the U.S. Army Corps of Engineers Coastal Field Data Collection program. The Chief of Engineers had granted permission for publication. This manuscript benefited significantly from the review comments of Falk Feddersen and Brian Parsons.

### LITERATURE CITED

- BEAVERS, R.L., 1999. Storm Sedimentation on the Surf Zone and Inner Continental Shelf, Duck, North Carolina. Durham, North Carolina: Duke University, Ph.D. thesis.
- BIRKEMEIER, W.A.; DEWALL, A.W.; GORBICS, C.S., and MILLER, H.C., 1981. A User's Guide to CERC's Field Research Facility. Fort Belvoir, Virginia: U.S. Army Corps of Engineers (USACE), Coastal Engineering Research Center. CERC Miscellaneous Report 81-7.
- DEAN, R.G. and DALRYMPLE, R.A., 1991. *Water Wave Mechanics for Engineers and Scientists*. Singapore: World Scientific, 353p.
- JONSSON, I.G., 1966. Wave boundary layers and friction factors. Proceedings of the 10th International Conference on Coastal Engineering (Tokyo, Japan, ASCE), pp. 127-148.
- LONGUET-HIGGINS, M.S.; CARTWRIGHT, D.E., and SMITH, N.D., 1963. Observations of the directional spectrum of sea waves using the motions of a floating buoy. *Ocean Wave Spectra*. Easton, Maryland: Prentice-Hall, pp. 111-131.
- MADSEN, O.S.; POON, Y., and GRABER, H.C., 1988. Spectral wave attenuation by bottom friction: theory. Proceedings of the 21st International Conference on Coastal Engineering (Delft, Netherlands, ASCE), pp. 492-504.
- NELSON, R.C., 1996. Field measurements of bed roughness for waves on an offshore reef. Proceedings of the 25th International Conference on Coastal Engineering (Orlando, Florida, ASCE), pp. 3143-3154.
- SMYTH, C. and HAY, A.E., 2002. Wave friction factors in nearshore sands. *Journal of Physical Oceanography*, 32, 3490-3498.
- SMYTH, C. and HAY, A.E., 2003. Near-bed turbulence and bottom friction during SandyDuck97. *Journal of Geophysical Research*, 108(C6), 3197-3210.
- TREMBANIS, A.C.; WRIGHT, L. D.; FRIEDRICHS, C. T.; GREEN, M. O., and HUME, T., 2003. The effects of spatially complex inner shelf roughness on boundary layer turbulence and current and wave friction: Tairua embayment, New Zealand. *Continental Shelf Research*, 24, 1549-1571.
- WRIGHT, L.D., 1995. *Morphodynamics of Inner Continental Shelves*. Boca Raton, Florida: CRC Press, 256 p.
- YOUNG, I.R., and GORMAN, R.M., 1995. Measurements of the evolution of ocean wave spectra due to bottom friction. *Journal of Geophysical Research*, 100(C6), 10987-11004.